

**Title**

Subtitle

**Max Sharnoff**

Trinity 2022

candidate number

MCompSci Computer Science



# Abstract

Detecting changes in human lung morphology and determining its effects on lung function requires significant time commitment per patient, so statistical analysis on many individuals is infeasible. Computational models of the lung are therefore a natural choice for researching the effects of altered lung morphology, with reference to existing lung function tests.

Accurate computational models also allow investigation into properties of the lungs that cannot feasibly be measured; e.g., increased internal stress in one location from damaged airways elsewhere.

This paper builds on recent advancements in modelling airflow in the lungs ([reference to Foy](#)) to produce an efficient, accurate model of the lungs that supports simple alterations to the simulated morphology. We then use this model to determine the strains placed on the rest of the lungs by various kinds of constricted or damaged airways.

# Contents

<b>1</b>	<b>Introduction</b>	<b>3</b>
1.1	Motivation . . . . .	3
1.2	Contributions to the field . . . . .	3
<b>2</b>	<b>Background</b>	<b>4</b>
2.1	Physiology of the lungs . . . . .	4
2.2	Clinical methods . . . . .	4
2.3	Prior computational models . . . . .	4
<b>3</b>	<b>Methods</b>	<b>5</b>
3.1	Simultaneous Equations . . . . .	5
3.2	Modelling in the Abstract . . . . .	6
3.3	Units & Modified Equations for Numerical Stability . . . . .	7
3.4	Sparse Matrices . . . . .	8
3.5	Procedural Lung Generation & Configuration . . . . .	8

# 1 Introduction

## 1.1 Motivation

Respiratory diseases account for more than 10% of *all* disability-adjusted life-years lost due to any medical condition, second only to cardiovascular diseases. [1] Because of this, any betterment of our understanding of the lungs and how they change from damage has immediate benefits towards understanding one of the most significant categories of disease.

In spite of this, there are relatively few existing methods for experimentation. Clinical observations on live patients are necessarily limited, and common techniques – spirometry, inert-gas washout, and fMRI imaging – all have severe limitations that render them infeasible or impossible to use for obtaining detailed data on the lungs at scale. And on top of that, the difficulty of drawing inference from these methods is enhanced by the fact that they are purely observational; in this paper, we are concerned with the effects of certain changes in lung morphology (such as: tightening of the airways, stiffness in the expansion and contraction, etc.).

Of course, it would be unethical to *induce* these changes in patients. However, sufficiently-accurate computational models present a natural solution. By designing models that can easily be arbitrarily deformed or otherwise altered, we create the opportunity to efficiently investigate how targeted changes in lung morphology affect both lung functioning as a whole and the stresses placed on individual regions.

**Todo:** I'd like to add something along the lines of: “historically, computational models have been too expensive for experimentation without specialized equipment, but recent developments (i.e. Foy) have show other methods for simulating airflow are both efficient and accurate.”

## 1.2 Contributions to the field

This paper introduces a new tool for simulating and observing changes to the lungs, and their precise effects.

**Todo:** Something about: “this is useful to people looking to find new results about *how* the lungs get impacted by various diseases.” Would like to also say: “we have investigated the effects of clinically-observed symptoms from a couple diseases, to showcase the utility of this tool”

## 2 Background

### 2.1 Physiology of the lungs

Basic points:

- air comes in through mouth, meets the lungs at the larynx
- lungs start off with the trachea, turns into bronchi/bronchial tubes
- eventually turns into bronchioles, alveoli & capillary network (although we don't care *as* much about these)

Want to talk about typical dimensions of each part here, as well as typical airflow & how that's observed (e.g. "what tests are used?") – talk about inert-gas washout, among others.

### 2.2 Clinical methods

- fMRI – typically very expensive & fairly low granularity: Good at getting an overview of the lung morphology, but resolution is typically low. (Not 100% sure how accurate this assessment is, but I think I saw something about it.)
- Inert gas washout

The above are good for *observing* changes in a patient, but have a couple shortcomings if we want to analyze the effects of lung morphology. Firstly, observational tests cannot be performed quickly; it would be prohibitively expensive to acquire the data for any kind of large-scale analysis. Secondly, current clinical methods do not allow forced changes to patient lung morphology (even without the risks and ethical considerations).

For those reasons, it is natural to turn to simulations – in particular, computational models – in order to gain insight into impact on physiology and overall function from isolated changes within the lungs.

### 2.3 Prior computational models

Talk briefly about proper fluid dynamics being too computationally expensive, use that to tie into the model from Foy.

There's definitely other models, still need to look into those.

### 3 Methods

Broadly speaking, this section comes in two parts; first defining the more theoretical underpinnings of the model used for simulation, followed by detail on the implementation in practice. There is relatively little theory to discuss; much of it comes from prior work.[2]

At a high level, we use a system of simultaneous equations to determine how the state of the simulated lungs evolves, updating in discrete timesteps to give a close approximation to the way a similar physical system would behave. Equation 4 governs the conservation of volume from one timestep to the next, which allows us to obtain greater numerical stability than we might otherwise, e.g., with  $\text{volume}_{t+1} = \text{volume}_t + \text{flow}dt$ .

Instead of a “full” fluid simulation (e.g., with the Navier-Stokes equations), we use a one-dimensional simulation as shown in (author?), (year?).

#### 3.1 Simultaneous Equations

This section provides a summary and brief description of the four simultaneous equations that govern the state of our system, the first of which is the following:

$$P_{\text{parent}(i)} - P_i = R(i)Q_i \quad (1)$$

This specifies that the pressure differential between the distal end of branch  $i$  and its parent must equal the pressure from the resistance from the flow through this branch  $i$ . For the “root” branch,  $P_{\text{parent}(i)}$  is the pressure at the trachea – typically atmospheric pressure.

The resistance term  $R(i)$  is defined as following function, as given by Pedley et al. (1970):

$$R(i) = \frac{2\mu L_i c}{\pi r_i^4} \left( \frac{4\rho |Q_i|}{\mu \pi L_i} \right)^{\frac{1}{2}}$$

The parenthesized term corresponds to the Reynold’s number of the flow, scaled by the ratio of the diameter of the branch to its length  $L_i$ .  $r_i$  is the radius of branch  $i$ ,  $\mu$  is the viscosity of the air, and  $c = 1.85$  is a correction constant.

The second equation ensures incompressibility; the flow through a bifurcation must equal the sum of the flow through its children:

$$Q_i = \sum Q_{\text{child}} \quad (2)$$

where each *child* refers to any branch  $c$  with  $\text{parent}(c) = i$ .

The third equation maintains that the volume of an acinar region changes with the flow into or out of it for the given timestep:

$$V_i^t = V_i^{t-1} + dtQ_i^t \quad (3)$$

where  $dt$  is the timestep size,  $t$  refers to the current timestep, and  $V_i$  is the volume of the acinar region of branch  $i$ .

The final equation defines the elastic force of each acinar region, relating the pressure it exerts on its branch to the volume of the region itself and the pressure outside it:

$$P_i = \frac{1}{C_i} V_i + P_{pl}(t) \quad (4)$$

where  $P_{pl}(t)$  is the pleural pressure (i.e. the “pressure” from the diaphragm, outside the acinar region) at the current time and  $C_i$  is the *compliance* of the acinar region of branch  $i$ . The pleural pressure changes over time to mimic human breathing patterns – hence why it is parameterised by  $t$ .

### 3.2 Modelling in the Abstract

We use an *implicit* Euler’s method to model the system as it progresses: at each timestep, our simulation updates its state to the value of an approximate solution to the system of equations above. Equation 4 provides the necessary bounds to make the method implicit, giving us higher accuracy at the cost of implementation complexity.

To solve for an approximate solution at each timestep, we use Newton’s method with  $f_{\mathbf{S}}(\mathbf{x})$  as defined below, iterating until  $\|f_{\mathbf{S}}(\mathbf{x})\|^2 \leq tol$  and  $\|dx\|^2 \leq tol$ , with a tolerance of  $10^{-6}$ . The two “inputs” –  $\mathbf{S}$  and  $\mathbf{x}$  – partition the state of the model into the variables that are controlled externally (e.g.: pleural pressure, compliance) and those that are calculated from the system state (e.g.: acinar volume, airflow). The definitions of  $\mathbf{x}$  and  $f_{\mathbf{S}}$  are given by:

$$x = (P_i..., Q_i..., V_i...) \\ f_{\mathbf{S}}(\mathbf{x}) = \begin{bmatrix} P_{\text{parent}(i)} - P_i - R(i)Q_i \\ \vdots \\ Q_i - \sum Q_{\text{child}} \\ \vdots \\ V_i^t - V_i^{t-1} - dtQ_i^t \\ \vdots \\ P_i - P_{pl}(t) - \frac{1}{C_i}V_i \\ \vdots \end{bmatrix}$$

Note that the values in  $\mathbf{x}$  and equations in  $f$  are repeated only as many times as fits; e.g., there are fewer acinar regions than total branches, so there are fewer components in  $\mathbf{x}$  from each  $V_i$  than from each  $Q_i$ .

As  $\mathbf{S}$  only exists in the abstract sense, we won’t bother to define its structure; all that’s necessary to know is that it contains every variable referred to in  $f$  that is not already given explicitly by  $\mathbf{x}$ .

It’s worth noting that in practice, the above definitions are only *nearly* correct; a few adjustments were made to the inputs and equations to mitigate limitations from floating-point accuracy. These are discussed in the next section.



### 3.3 Units & Modified Equations for Numerical Stability

It is worth making explicit the units used for each value in our simultaneous equations. After careful consideration, these were considered to provide the best trade-off of familiar units and those with values of magnitude close to one, where floating-point accuracy is maximized. As we will see momentarily, the spread was still quite wide. The chosen units were:

Type of thing ???	Units
Distance	m
Volume	m <sup>3</sup>
Flow velocity	$\frac{\text{m}^3}{\text{s}}$
Density	$\frac{\text{kg}}{\text{m}^3}$
Pressure	Pascals $\left(\frac{\text{kg}}{\text{m}\cdot\text{s}^2}\right)$
Compliance	$\frac{\text{m}^3}{\text{Pascal}} \left(\frac{\text{m}^4\cdot\text{s}^2}{\text{kg}}\right)$
Resistance	$\frac{\text{kg}}{\text{m}^4\cdot\text{s}}$
Viscosity	$\frac{\text{kg}}{\text{m}\cdot\text{s}}$

One of the challenges with using these units is that some values are at a much greater magnitude than the others. For example, the pressure inside each branch is close to atmospheric pressure – or about  $10^5$  Pascals, but pressure *gradients* are typically much smaller.

In practice, this can mean that if the  $dx$  from our Euler step is too small, the pressure won't change; it doesn't have the necessary precision at that magnitude.

To mitigate this issue, we define two new values:  $\hat{P}$  and  $\hat{V}$ , which are given by:

$$\hat{P} = P - P_{\text{atm}} \quad (5)$$

where  $P_{\text{atm}}$  is atmospheric pressure; and:

$$\hat{V} = V - V|_{P=P_{\text{atm}}} \quad (6)$$

$$= C(\hat{P} - P_{pl}) \quad (7)$$

Note that the definition of  $\hat{V}$  would be the result of simply substituting  $\hat{P}$  for  $P$  in 4. Applying these substitutions gives the following equations, equivalent to their counterparts above:

$$\hat{P}_{\text{parent}} - \hat{P}_i = R(i)Q_i \quad (8)$$

$$Q_i = \sum Q_{\text{child}} \quad (9)$$

$$\hat{V}_i^t = \hat{V}_i^{t-1} + dt Q_i^t \quad (10)$$

$$\hat{P}_i = \frac{1}{C_i} \hat{V}_i + P_{pl}(t) \quad (11)$$

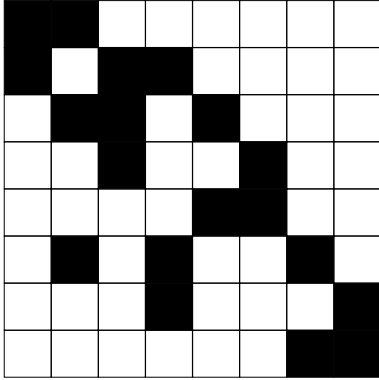
Representing the pressure and volume by their *offset* from values at atmospheric pressure causes them to cluster much closer to zero – the magnitude of the mean is significantly decreased, relative to the variance of the values. This of course greatly improves the accuracy of each Euler step.

Note: The same substitutions also apply to our representations of the state of the model & the optimization function used for Newton’s method, as shown in subsection 3.2.

### 3.4 Sparse Matrices

A key observation that can aid in simulation speed is that we can represent the Jacobean of our optimization function  $f$  in  $\mathcal{O}(n)$  space using sparse matrices – which is necessary to allow simulation of the lungs up to a high depth without a quadratic blow-up in runtime.

**Todo:** In order to flesh this out, it would be good to clarify whether there’s any advantage to be gained from LU decomposition (or otherwise) when using this sparse representation. I’m actually not currently sure that that’s true- which would negate a lot of the potential benefit for these sparse matrices.



### 3.5 Procedural Lung Generation & Configuration

**Todo:** This section will generally talk about the JSON configuration file that allows us to define the structure of the lung & schedule degradation.

## References

- [1] The global impact of respiratory disease – second edition.
- [2] BH Foy. Computational models of pulmonary function tests, 2018.